

Search for  $C$  Violation in  $\eta \rightarrow \pi^+\pi^-\pi^0$ †

COLUMBIA-BERKELEY-PURDUE-WISCONSIN-YALE COLLABORATION\*

(Received 12 May 1966)

We have searched for charge asymmetry in the decay distribution of our combined sample of 1300  $\eta$  decays. We divide the Dalitz plot into six azimuthal sectors, where sectors 1, 2, and 3 are the charge conjugates of sectors 6, 5, and 4, respectively. We find  $R = (N_1 + N_2 + N_3 - N_4 - N_5 - N_6)/N_{\text{total}} = +0.058 \pm 0.034$ , and  $R' = (N_1 - N_2 + N_3 - N_4 + N_5 - N_6)/N_{\text{total}} = +0.068 \pm 0.033$ . A more detailed parametrization is also given; it yields results consistent with those for  $R$  and  $R'$ . The largest theoretical estimates give about 5% for  $R$ . Thus our observed asymmetry admits the possibility of a  $C$  violation as large as the theoretical maximum. Since the asymmetry differs from zero by only two standard deviations, we can reach no definite conclusion.

## I. INTRODUCTION

WE present here the results of a search for charge asymmetry in the decay

$$\eta \rightarrow \pi^+\pi^-\pi^0. \quad (1)$$

The sample, which contains 1300  $\eta \rightarrow \pi^+\pi^-\pi^0$ , is obtained by combining our individual experiments. Table I summarizes the reactions in which the  $\eta$  are produced and lists the groups responsible for each experiment.<sup>1</sup>

It has been suggested<sup>2</sup> that the observed violation of  $CP$  invariance in  $K_2 \rightarrow \pi^+\pi^-$  is not due to the weak interaction, but may be due to a  $C$  and  $T$  noninvariant interaction for which the square of the coupling constant is about  $10^{-2}$  times that of the strong interaction. Such an interaction could also be the result of very large  $C$  and  $T$  violations of the hadronic electromagnetic interaction.<sup>3</sup> The decay (1) occurs through virtual

electromagnetic interactions; therefore, it provides a natural test of these hypotheses.<sup>4</sup> Detection of a charge asymmetry in the energy distribution of the  $\pi^+$  and  $\pi^-$  would constitute an absolute proof of  $C$  noninvariance in  $\eta$  decay. However, because there is no real photon in reaction (1), one cannot determine whether or not the  $C$ -noninvariant interaction (if it exists) is of electromagnetic origin. The magnitude of the asymmetry (if it exists) has been theoretically estimated to be no larger than about 5%.<sup>5</sup>

## II. SUMMARY OF RESULTS

A. Test of the  $C$ -Invariance Hypothesis

If the Dalitz plot of the 1300 events is divided into six "azimuthal" sectors [Fig. 1(a)] and if  $\chi^2$  is calculated for the hypothesis "no charge asymmetry," we find

$$\chi^2 = 5.52, \quad (2)$$

where  $\chi^2 = 3$  is expected. This corresponds to a  $\chi^2$  probability of 15%. To this confidence level *our results are consistent with the absence of  $C$  violation.*

B. Tests of the  $C$ -Noninvariance Hypothesis

1. The "plus-minus" asymmetry of the Dalitz plot is

$$R \equiv \frac{(\eta_1 - \eta_6) + (\eta_2 - \eta_5) + (\eta_3 - \eta_4)}{\eta_1 + \eta_2 + \eta_3 + \eta_4 + \eta_5 + \eta_6} = 0.058 \pm 0.034, \quad (3)$$

where  $\eta_i$  is the corrected number of  $\eta$  decays in sector  $i$  of the Dalitz plot. (See Table VII.)

2. The "alternating plus-minus" asymmetry of the Dalitz plot is

$$R' \equiv \frac{(\eta_1 - \eta_6) - (\eta_2 - \eta_5) + (\eta_3 - \eta_4)}{\eta_1 + \eta_2 + \eta_3 + \eta_4 + \eta_5 + \eta_6} = +0.068 \pm 0.033. \quad (4)$$

3. Account can be taken of the specific radial and azimuthal variation of the plus-minus asymmetry. For

<sup>4</sup> R. Friedberg, T. D. Lee, and M. Schwartz (unpublished).

<sup>5</sup> T. D. Lee, Phys. Rev. **139**, B1415 (1965) estimates  $\leq 5\%$ ; S. L. Glashow and C. M. Sommerfield, Phys. Rev. Letters **15**, 78 (1965) estimate  $\leq 1\%$ ; M. Nauenberg, Phys. Letters **17**, 329 (1965), and B. Barrett, M. Jacob, M. Nauenberg, and T. N. Truong, Phys. Rev. **141**, 1342 (1966) estimate  $\leq 3\%$ .

\* Members of the collaboration are: C. Baltay, P. Franzini, G. Lütjens, M. Schwartz, J. C. Severiens, and D. Zanello; Columbia University, New York, New York. F. S. Crawford, Jr., S. M. Flatté, E. C. Fowler, G. Goldhaber, S. Goldhaber (deceased), R. A. Grossman, L. J. Lloyd, L. R. Price, B. Shen, F. T. Solmitz, and M. L. Stevenson; Lawrence Radiation Laboratory, University of California, Berkeley, California. F. Loeffler, R. MacIlwain, and M. Meer; Purdue University, Lafayette, Indiana. M. Foster, M. Good, R. Hartung, R. Matsen, M. Peters, and D. Reeder; University of Wisconsin, Madison, Wisconsin. H. W. J. Foelsche, F. James, J. Johnson, and H. Kraybill, Yale University, New Haven, Connecticut.

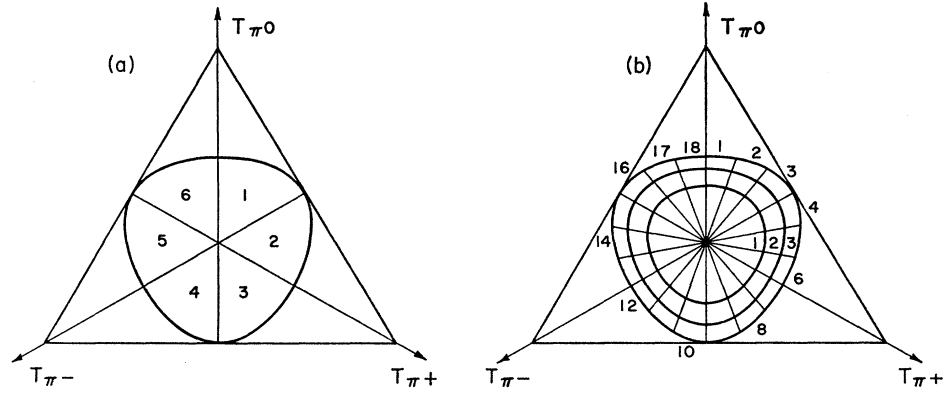
† This work was done under the auspices of the U. S. Atomic Energy Commission.

<sup>1</sup> The individual experiments, with code numbers that correspond to the tables, are No. 1: C. Baltay, P. Franzini, G. Lütjens, J. C. Severiens, D. Tycko, and D. Zanello, Phys. Rev. **145**, 1103 (1966); No. 2: C. Alff, D. Berley, D. Colley, N. Gelfand, U. Nauenberg, D. Miller, J. Schultz, J. Steinberger, T. H. Tan, H. Brugger, P. Kramer, and R. Plano, Phys. Rev. Letters **9**, 322 (1962); No. 3: M. Foster, M. Peters, R. Hartung, R. Matsen, D. Reeder, M. Good, M. Meer, F. Loeffler, and R. MacIlwain, Phys. Rev. **138**, B652 (1965); No. 4: H. W. J. Foelsche and H. Kraybill, Phys. Rev. **134**, B1138 (1964); No. 5: F. James and H. Kraybill, Phys. Rev. **142**, 896 (1966); No. 6: J. Johnson and H. Kraybill (to be published); No. 7: F. S. Crawford, Jr., E. C. Fowler, R. A. Grossman, L. J. Lloyd, and L. R. Price, Phys. Rev. Letters **11**, 564 (1963); **13**, 421 (1964); and to be published; No. 8: G. Goldhaber, S. Goldhaber, and B. Shen (to be published); No. 9: M. L. Stevenson, F. T. Solmitz, and S. M. Flatté (to be published).

<sup>2</sup> T. D. Lee and L. Wolfenstein, Phys. Rev. **138**, B1490 (1965); L. Okun (to be published); J. Prentki and M. Veltman, Phys. Letters **15**, 88 (1965).

<sup>3</sup> J. Bernstein, G. Feinberg, and T. D. Lee, Phys. Rev. **139**, B1650 (1965).

FIG. 1. Dalitz plot sectors. (a) 6 sectors. (b) 54 ( $18 \times 3$ ) sectors.



this purpose we divide the Dalitz plot into 54 sectors [Fig. 1(b)] and fit to a  $C$ -conserving complex linear matrix element plus a  $C$ -nonconserving matrix element. The  $C$ -violating amplitude can arise both from  $\Delta I=0$  and  $\Delta I=2$  transitions. (The asymmetry ratio  $R$  emphasizes the  $\Delta I=2$  part;  $R'$  emphasizes the  $\Delta I=0$  part.) We find the  $C$ -nonconserving amplitude to be two standard deviations from zero if the  $C$  violation occurs only in the  $\Delta I=0$  transition, and one standard deviation from zero if the  $C$  violation occurs only in the  $\Delta I=2$  transition.

Our results therefore admit the possibility of a  $C$  violation as large as the theoretical maximum.<sup>5</sup> However no definite conclusion can be drawn from the available data.

### III. EXPERIMENTAL DETAILS

The remainder of this paper contains the details of our analysis. The individual experiments are listed in Table I and Ref. 1. The  $\eta$  mesons are produced in the reactions

$$\pi^\pm p \rightarrow \pi_a^\pm p \eta, \quad \eta \rightarrow \pi_b^\pm \pi^\mp \pi^0, \quad (5)$$

$$K^- p \rightarrow \Lambda \eta, \quad \Lambda \rightarrow p \pi^-, \quad \eta \rightarrow \pi^+ \pi^- \pi^0, \quad (6)$$

and

$$\bar{p} p \rightarrow \pi^+ \pi^- \eta, \quad \eta \rightarrow \pi^+ \pi^- \pi^0. \quad (7)$$

Typical three-pion mass distribution for these reactions are displayed in Fig. 2.

#### A. "Low Momentum" $\pi^+ p$ Experiments

Experiments 3, 4, and 7 of Table I correspond to reaction (5). They have less than 3% background and have  $\eta \rightarrow \pi^+ \pi^- \gamma$  removed. No background subtractions were made for these experiments. These experiments have been corrected for a spurious charge asymmetry that results from picking the wrong pion in the ambiguous events (which amount to about 15%) where either  $\pi_a$  or  $\pi_b$  can combine with the other two (unambiguous) pions to give the correct  $\eta$  mass. We used the event-simulating program FAKE<sup>6</sup> to calculate the induced bias, and obtained the corrections shown in Table II; the average spurious asymmetry is  $R=+0.013$ , or  $R'=+0.02$ . Table III gives the corrected number of events in each of the six sectors of the Dalitz plot. We first test the hypothesis "no charge asymmetry" with

TABLE I. Details of compilation. (See also Ref. 1.)  $\eta$  is the approximate number of  $\eta$ 's above background.  $f_{BG}=BG/(\eta+BG)$  is the fractional background in the  $\eta$  mass region.  $f_{AMB}$  is the fraction of events in the  $\eta$  mass region that have an ambiguous pion.

Expt. No.	Group	Reaction	Momentum (BeV/c)	$\eta$	$f_{BG}$	$f_{AMB}$
1	Colum.	$\bar{p} + p \rightarrow \pi^+ \pi^- + (\eta \rightarrow \pi^+ \pi^- \pi^0)$	0	149	0.52	...
2	Colum.	$\pi^+ + p \rightarrow p \pi_a^+ + (\eta \rightarrow \pi_b^+ \pi^- \pi^0)$	2.5	47	0.36	0.08
3a	Wis.-Pur.		1.225	134	0.02	0.16
3b	Wis.-Pur.		1.275	140	0.02	0.13
4a	Yale		1.225	78	0.03	0.14
4b	Yale		1.395	74	0.03	0.09
5	Yale		2.08	43	0.37	0.16
6	Yale		1.76	55	0.35	0.16
7a	LRL		1.05	41	0.02	0.10
7b	LRL		1.17	113	0.02	0.21
8a	LRL	3.7	33	0.27	0.03	
				(Subtotal=758)		
7c	LRL	$\pi^- + p \rightarrow p \pi_a^- + (\eta \rightarrow \pi_b^+ \pi^- \pi^0)$	1.17	60	0.02	0.20
8b	LRL		3.7	9	0.50	0.11
				(Subtotal=69)		
9	LRL	$K^- + p \rightarrow \Lambda + (\eta \rightarrow \pi^+ \pi^- \pi^0)$	1.2 to 1.8	309	0.31	0

<sup>6</sup> G. R. Lynch, Lawrence Radiation Laboratory Report UCRL-10335, 1962 (unpublished).

TABLE II. Number of events to be added to each of the six sectors for the “wrong pion” correction in experiments 3, 4, and 7.

Experiment No.	Number of events					
	Sector 1	Sector 2	Sector 3	Sector 4	Sector 5	Sector 6
3a	-0.87±0.70	-0.90±0.44	0.30±0.70	2.26±1.1	0.28±0.33	-1.05±0.44
3b	-0.85±0.29	-0.23±0.40	0.18±0.35	0.96±0.40	0.14±0.20	-0.20±0.18
4a	-0.44±0.35	-0.45±0.72	0.15±0.35	1.13±0.53	0.14±0.17	-0.53±0.22
4b	-0.35±0.12	-0.17±0.11	0.17±0.16	0.24±0.18	0.24±0.14	-0.10±0.13
7a	-0.06±0.04	0.00±0.03	0.02±0.04	0.08±0.06	0.04±0.06	-0.08±0.05
7b	-0.83±0.31	-0.69±0.31	0.65±0.36	0.79±0.36	0.50±0.14	-0.37±0.12
7c	0.38±0.14	0.26±0.16	-0.26±0.17	-0.35±0.17	-0.26±0.07	0.20±0.06
Totals	-3.02±0.91	-2.18±1.00	+1.21±0.96	+5.11±1.36	+1.08±0.48	-2.13±0.56

a  $\chi^2$  test:

$$\chi^2 = \frac{(\eta_1 - \eta_6)^2}{\sigma_{16}^2} + \frac{(\eta_2 - \eta_5)^2}{\sigma_{25}^2} + \frac{(\eta_3 - \eta_4)^2}{\sigma_{34}^2}, \quad (8)$$

where  $\eta_i$  is the corrected number of etas in sector  $i$ , and

$$\sigma_{ij}^2 = (\delta\eta_i)^2 + (\delta\eta_j)^2, \quad (9)$$

with

$$(\delta\eta_i)^2 = \eta_i \quad (10)$$

for these experiments. We also calculate the asymmetries  $R$  and  $R'$  as defined in Eqs. (3) and (4). For the 640 decays of experiments 3, 4, and 7 the results are

$$\chi^2 = 2.05, \quad R = +0.041 \pm 0.040, \\ \text{and } R' = +0.051 \pm 0.040. \quad (10a)$$

### B. “High Momentum” $\pi + p$ Experiments

Experiments 2, 5, 6, and 8 also correspond to reaction (5), but at considerably higher beam momentum than experiments 3, 4, and 7. The fraction  $f_{BG} = BG/(BG + \eta)$  of non- $\eta$   $\pi^+\pi^-\pi^0$  background in the  $\eta$  mass region is not negligible. [A typical mass plot is shown in Fig. 2(b).] This background is not expected to have charge symmetry, and must be calculated and subtracted separately for each sector of the Dalitz plot. The background is subtracted as follows. First, all events are removed which satisfy  $\omega^0 \rightarrow \pi^+\pi^-\pi^0$ . For each experiment and for each sector  $i$ , let  $N_i$  denote the number of events in the  $\eta$ -mass band, with the  $\pi^+\pi^-\pi^0$  mass lying

TABLE III. Corrected number of events in each of the six sectors for experiments 3, 4, and 7.

Experiment No.	Number of events						Total
	Sector 1	Sector 2	Sector 3	Sector 4	Sector 5	Sector 6	
3a	14.13	15.10	38.30	34.26	19.28	12.95	134.02
3b	13.15	24.77	45.18	27.96	19.14	9.80	140.00
4a	16.56	8.55	22.15	12.13	10.14	8.47	78.00
4b	6.65	10.83	18.17	20.24	10.24	7.90	74.03
7a	3.94	8.00	9.02	8.08	8.04	3.92	41.00
7b	8.17	17.31	25.65	29.79	20.50	11.63	113.05
7c	3.38	8.26	15.74	17.65	8.74	6.20	59.97
Totals	65.98	92.82	174.21	150.11	96.08	60.87	640.07

between 530 and 570 MeV for experiments 2, 6, and 8, and between 535 and 570 MeV for experiment 5. Let  $C_i$  denote the total number of events in the two neighboring background-sampling bands with  $\pi^+\pi^-\pi^0$  mass from 500 to 530 and 570 to 600 MeV (the authors of experiment 5 used 505 to 535 and 570 to 600 MeV). We next draw a smooth curve for what we think should be the background behavior in the control and peak regions and determine the number of background events, BG, that lie in the peak region. The number of events in both control regions is  $\sum C_i$ . For all experiments this curve is nearly a straight line. Let  $b \equiv BG/\sum C_i$  denote the ratio of the background events to the control events. Since the background curve is nearly a straight line,  $b$  can be expressed as the ratio of the width of the peak region to the total width of the control regions. Thus

$$b = (570 - 535 = 35) / [(600 - 570 = 30) + (530 - 500 = 30)].$$

We then take the corrected number of  $\eta$  events in the  $\eta$  band to be

$$\eta_i = N_i - bC_i \quad (11)$$

with a standard deviation

$$(\delta\eta_i)^2 = N_i + b^2C_i. \quad (12)$$

The average fractional background  $f_{BG} = bC_i/N_i$  is about 0.35 in these experiments. The decays  $\eta^0 \rightarrow \pi^+\pi^-\gamma$  cannot be separated out and removed. The fraction of events with an ambiguous pion is  $f_{AMB} \approx 0.11$ . No correction was made for the spurious asymmetry induced by the pion ambiguity. Table IV gives  $N_i$ ,  $C_i$ ,  $\eta_i$ , and  $(\delta\eta_i)^2$  for each experiment. We combine these experiments to obtain 178  $\eta$  events above background. We calculate  $\chi^2$  using Eqs. (8) and (9), and using Eq. (12) in place of (10). We also calculate  $R$  and  $R'$ . The results for experiments 2, 5, 6, and 8 are

$$\chi^2 = 0.81, \quad R = +0.041 \pm 0.102, \\ \text{and } R' = +0.010 \pm 0.103. \quad (13)$$

### C. $\bar{p} + p$ Experiment

Experiment 1 corresponds to reaction (7). The fractional background is  $f_{BG} \approx 0.52$ . A three-pion mass plot

is shown in Fig. 2(c). The non-eta pion production has been verified in detail to be charge symmetric,<sup>7</sup> as is expected if the initial  $\bar{p}p$  system is an incoherent mixture of eigenstates of charge conjugation, and charge conjugation is conserved in strong interactions. Thus the pion ambiguity introduces no spurious asymmetry. We take advantage of the known charge symmetry of the background and assume that sectors 1 and 6 have the same expected background, and similarly for sectors 2 and 5, and for 3 and 4. The  $\eta$  band used by these experimenters is from 535 to 565 MeV. The two background-sampling bands are from 500 to 535 and 565 to 600 MeV. Thus we have  $b=30/70$ . The corrected numbers of  $\eta$  decays in sectors 1 and 6 are given by

$$\eta_1 = N_1 - \frac{1}{2}b(C_1 + C_6), \quad (14)$$

and

$$\eta_6 = N_6 - \frac{1}{2}b(C_1 + C_6),$$

with standard deviations and correlation

$$(\delta\eta_1)^2 = N_1 + \frac{1}{4}b^2(C_1 + C_6), \quad (15)$$

$$(\delta\eta_6)^2 = N_6 + \frac{1}{4}b^2(C_1 + C_6), \quad (16)$$

and

$$\delta\eta_1\delta\eta_6 = \frac{1}{4}b^2(C_1 + C_6). \quad (17)$$

TABLE IV. Data for experiments 2, 5, 6, and 8.

Experiment No.	$b$	Sector	$N_i$	$C_i$	$\eta_i$	$(\delta\eta_i)^2$
2	40/60	1	9	6	5.00	11.67
		2	14	10	7.33	18.44
		3	18	3	16.00	19.33
		4	14	8	8.67	17.56
		5	11	6	7.00	13.67
		6	7	6	3.00	9.67
5	35/60	1	6	12	-1.00	10.08
		2	13	7	8.92	15.38
		3	20	6	16.50	22.04
		4	15	11	8.58	18.74
		5	8	1	7.42	8.34
		6	6	7	1.92	8.37
6	40/60	1	10	8	4.67	13.56
		2	20	7	15.33	23.11
		3	18	10	11.33	22.44
		4	20	3	18.00	21.33
		5	12	9	6.00	16.00
		6	5	8	-0.33	8.56
8a	40/60	1	6	2	4.67	6.89
		2	6	5	2.67	8.22
		3	9	4	6.33	10.78
		4	13	2	11.67	13.89
		5	8	2	6.67	8.89
		6	3	3	1.00	4.33
8b	40/60	1	1	1	0.33	1.44
		2	1	4	-0.66	2.78
		3	3	5	-0.33	5.22
		4	7	2	5.67	7.89
		5	4	2	2.67	4.89
		6	2	2	0.67	2.89

<sup>7</sup>C. Baltay, N. Barash, P. Franzini, N. Gelfand, L. Kirsch, G. Lütjens, J. C. Severiens, J. Steinberger, D. Tycko, and D. Zanillo, Phys. Rev. Letters **15**, 591 (1965).

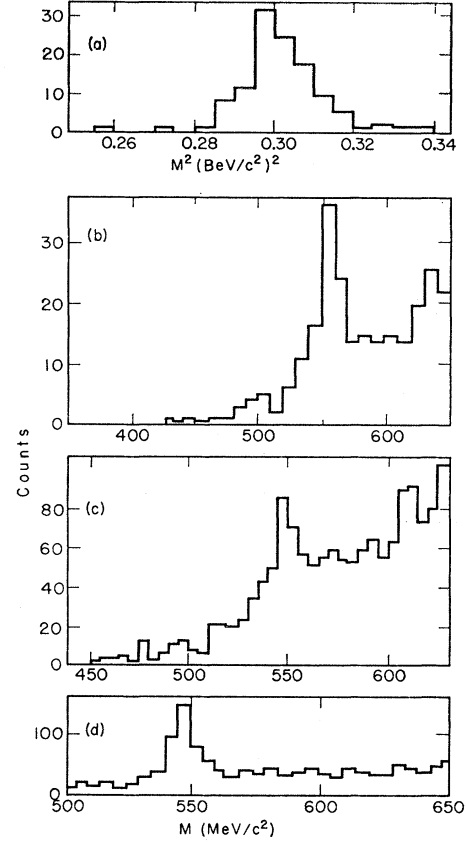


FIG. 2. Typical mass distributions. (a) Low-momentum (1170 MeV/c)  $\pi^+p \rightarrow \pi^+p\pi^+\pi^-\pi^0$ ; distribution in  $m^2(\pi^+\pi^-\pi^0)$ , with that  $\pi^+$  chosen which gives  $m^2(\pi^+\pi^-\pi^0)$  closest to 0.30 (BeV)<sup>2</sup>. The graph includes all events. (b) High-momentum (1.95 BeV/c)  $\pi^+p \rightarrow \pi^+p\pi^+\pi^-\pi^0$ ; distribution in  $m(\pi^+\pi^-\pi^0)$ , with each event plotted twice (once for each  $\pi^+$ ). Most events are not shown; they have larger mass than the upper limit (650 MeV) of the graph. (c) Stopping antiprotons,  $\bar{p}p \rightarrow \pi^+\pi^-\pi^+\pi^-\pi^0$ ; distribution in  $m(\pi^+\pi^-\pi^0)$ , with each event plotted four times. Most events have larger mass than the upper limit shown. (d)  $K^-p \rightarrow \Lambda\pi^+\pi^-\pi^0$ ; distribution in  $m(\pi^+\pi^-\pi^0)$ . Most events lie above the 650-MeV limit shown.

Similar relations hold for sectors 2 and 5, and for 3 and 4. Table V gives these quantities for each sector. The results of experiment 1 with 149  $\eta$  events above background are

$$\chi^2 = 5.23, \quad R = +0.040 \pm 0.120, \\ \text{and } R' = +0.094 \pm 0.119, \quad (18)$$

TABLE V. Data for experiment 1.

Sector	$N_i$	$C_i$	$\eta_i$	$(\delta\eta_i)^2$	$\delta\eta_i\delta\eta_j$
1	32	74	3.07	38.20	+6.20
6	43	61	14.07	49.20	
2	55	64	27.57	60.88	+5.88
5	59	64	31.57	64.88	
3	74	71	47.00	79.78	+5.78
4	53	55	26.00	58.78	

TABLE VI. Data for experiment 9.

Sector	$N_i$	$C_i$	$\eta_i$	$(\delta\eta_i)^2$
1	55	37	36.50	64.25
2	73	54	46.00	86.50
3	113	47	89.50	124.75
4	96	53	69.50	109.25
5	67	38	48.00	76.50
6	46	53	19.50	59.25

where  $\chi^2$  is given by Eq. (8), with

$$\sigma_{16}^2 = (\delta\eta_1)^2 + (\delta\eta_6)^2 - 2\delta\eta_1\delta\eta_6, \quad (19)$$

and similar expressions for  $\sigma_{25}$  and  $\sigma_{34}$ .

#### D. $K^-+p$ Experiment

Experiment 9 corresponds to reaction (6). There is no pion ambiguity. A mass plot is shown in Fig. 2(d). The  $\pi^+\pi^-\gamma$  contamination fraction  $(\eta \rightarrow \pi^+\pi^-\gamma)/(\eta \rightarrow \pi^+\pi^-\pi^0)$  is less than 8% for this sample of  $\eta$ s. The fractional background is  $f_{BG} \approx 0.31$  and is subtracted by the method discussed just before Eqs. (11) and (12). The  $\eta$  band is from 530 to 565 MeV. The background-sampling bands are from 495 to 530 and 565 to 600 MeV. Therefore  $b$  is 35/70. Table VI gives  $N_i$ ,  $C_i$ ,  $\eta_i$ , and  $(\delta\eta_i)^2$ . The results of experiment 9 with 309  $\eta$ 's above background are

$$\chi^2 = 4.07, \quad R = +0.113 \pm 0.074, \\ \text{and } R' = +0.126 \pm 0.074. \quad (20)$$

#### E. Combined Experiments

We finally combine the four subclasses of experiments—Nos. 3, 4, and 7; Nos. 2, 5, 6, and 8; No. 9; and No. 1—using the method of least squares on the results (10), (13), (18), and (20). To test the hypothesis “no charge asymmetry in any of the conjugate-sector pairs in any of the experiments,” we add the individual  $\chi^2$  values and obtain

$$\chi^2 = 12.15, \quad \text{with } \langle \chi^2 \rangle = 12. \quad (21)$$

This has a  $\chi^2$  probability of 0.4. We also calculate a weighted average of  $R$  and a weighted average of  $R'$ . We find

$$R_{av} = +0.055 \pm 0.032, \quad R'_{av} = +0.064 \pm 0.032. \quad (22)$$

TABLE VII. Combined data from all experiments.

Sector	$\eta_i$	$(\delta\eta_i)^2$	$\delta\eta_i\delta\eta_j$
1	119.22	212.07	+6.20
6	101.02	203.15	
2	198.98	308.14	+5.88
5	205.40	289.24	
3	360.54	458.67	+5.78
4	298.19	397.56	

 TABLE VIII. Entire sample of 1301.9 events divided into 20 equal bins in  $y$ . Increasing bin number corresponds to increasing  $y$ . The kinetic energy  $T_{\pi^0}$  is proportional to  $y$ .

$y$ bin	$N_\eta$	$(\delta N_\eta)^2$
1	27.88	38.69
2	67.23	80.38
3	92.24	108.54
4	81.67	103.28
5	102.76	136.27
6	86.58	120.14
7	90.24	126.42
8	104.43	140.04
9	84.08	126.91
10	83.67	124.18
11	86.88	119.05
12	81.11	121.10
13	76.61	110.44
14	37.83	80.61
15	45.71	82.99
16	40.83	82.65
17	50.35	75.31
18	27.82	54.28
19	19.00	41.87
20	15.00	28.30

(The  $\chi^2$  test takes no account of the fact that the four individual values happen to have the same sign.)

Instead of combining the results from the four subclasses of experiments, we can combine their data to obtain the total corrected number of  $\eta$ 's in each sector. The combined data are shown in Table VII. It gives the results already presented in Eqs. (2), (3), and (4).

#### IV. THEORETICAL MODELS: FIT TO THE COMBINED DATA

Although we cannot establish the existence of an asymmetry, neither can we rule out an asymmetry as large as the theoretical maximum.<sup>5</sup> It is therefore of interest to *assume*  $C$  noninvariance and parametrize the decay matrix element with a simple phenomenological model.<sup>5</sup> For the  $C$ -conserving part  $F$  of the matrix element we assume a complex linear matrix element

$$F = C(1 + \alpha\gamma), \quad \alpha = \alpha_R + i\alpha_I, \quad (23)$$

where  $C$  is a positive real normalization constant. For the  $C$ -nonconserving part  $f$  of the matrix element we assume

$$f = f_0 + f_2, \quad (24)$$

where  $f_0$  and  $f_2$  correspond to three-pion  $I$  spin 0 and 2, respectively. We assume<sup>5</sup>

$$f_0 = c_0 A_0 r^3 \sin 3\theta = c_0 A_0 x (3y^2 - x^2) \quad (25)$$

and

$$f_2 = c_2 A_2 r \sin \theta = c_2 A_2 x, \quad (26)$$

where  $c_2$  and  $c_0$  are positive real normalization constants and where

$$x = r \sin \theta = \sqrt{3}(T_+ - T_-)/Q \quad (27)$$

and

$$y = r \cos \theta = (3T_0 - Q)/Q \quad (28)$$

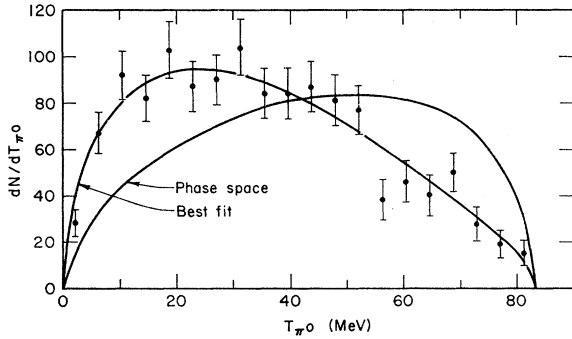


FIG. 3. Energy distribution of  $\pi^0$  in  $\eta \rightarrow \pi^+\pi^-\pi^0$ . The plotted points are from Table VIII. The two smooth curves correspond to phase space, and to the complex linear-matrix-element model, Eq. (29), using the best-fit parameters, Eq. (30).

are the Dalitz-plot coordinates. The complete matrix element is  $F+f$ . In the absence of final-state interactions among the three pions,  $CPT$  invariance (with a phase convention) requires that the  $C$ -conserving amplitude  $F$  be real, and the  $C$ -nonconserving amplitude  $f$  be pure imaginary.<sup>5</sup> Thus if we write  $A = A_R + iA_I$  for either  $A_0$  or  $A_2$ , absence of final-state interactions implies  $\alpha_I = A_R = 0$ , and hence, that  $|F+f|^2$  has no term odd in  $x$ , i.e., no charge asymmetry. In that case  $C$  noninvariance could not be established.

We first find  $\alpha$ . We integrate over  $x$  so that the interference term in  $|F+f|^2$  integrates to zero. We also assume  $|f|^2$  can be neglected compared to  $|F|^2$ . For fixed  $y$  the differential counting rate  $dN/dy$  is given by

$$\frac{dN}{dy} = |F|^2 \int_{\min}^{\max} dx = \frac{4\sqrt{3}pq}{Qm_{12}} |C|^2 [1 + 2\alpha_R y + (\alpha_R^2 + \alpha_I^2)y^2], \quad (29)$$

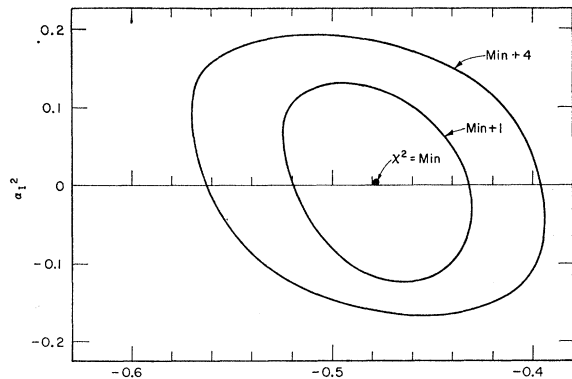


FIG. 4.  $\chi^2$  contour plot for complex linear-matrix-element parameters  $\alpha_R$  and  $\alpha_I^2$  of Eq. (29), obtained from data plotted in Fig. 3. Negative values for  $\alpha_I^2$  would correspond to an inadequacy in the linear-matrix-element parametrization, Eq. (23), and would call for a quadratic matrix element. We see that the linear matrix element is adequate, but that  $\alpha_I^2$  is poorly determined. The best-fit parameters of Eq. (30) correspond to the minimum  $\chi^2$ ; their errors correspond to  $\chi_{\min}^2 + 1$ .

where  $m_{12}$  is the mass of the  $\pi^+\pi^-$  dipion,  $p$  is the momentum of the  $\pi^0$  in the  $\eta^0$  rest frame, and  $q$  is the momentum of the  $\pi^+$  in the  $\pi^+\pi^-$  c.m. system. We find  $\alpha_R$  and  $\alpha_I^2$  by fitting Eq. (29) to the entire sample, histogrammed in 20 equal bins in  $y$ , as given in Table VIII. The data of Table VIII and the best fit to (29) are shown in Fig. 3. The  $\chi^2$  contour plot for  $\alpha_R$  and  $\alpha_I^2$  is shown in Fig. 4. (Negative values of  $\alpha_I^2$  would correspond to incompatibility with the assumption that a linear matrix element suffices to represent the data.)

TABLE IX. Numbers of events and squares of the errors in each of the 54 sectors.

Angular zone	Radial zone	$N$	$(\delta N)^2$
1	3	5.16	14.84
1	2	8.16	14.38
1	1	23.21	35.56
2	3	8.16	14.16
2	2	26.52	31.18
2	1	15.66	29.11
3	3	5.02	14.50
3	2	17.16	24.25
3	1	26.66	39.08
4	3	13.47	23.60
4	2	17.85	28.57
4	1	37.56	56.56
5	3	10.00	20.24
5	2	22.28	32.03
5	1	30.04	43.39
6	3	19.52	28.07
6	2	20.26	30.07
6	1	33.54	49.46
7	3	32.78	39.17
7	2	25.56	30.29
7	1	43.78	56.52
8	3	38.85	46.53
8	2	38.19	49.16
8	1	28.97	39.68
9	3	51.78	64.52
9	2	52.96	63.77
9	1	52.42	69.86
10	3	46.96	56.10
10	2	45.64	55.58
10	1	33.73	49.48
11	3	36.28	44.65
11	2	31.04	39.58
11	1	35.48	46.60
12	3	22.54	26.68
12	2	19.33	29.14
12	1	34.71	47.40
13	3	22.38	30.37
13	2	23.91	30.20
13	1	31.24	42.59
14	3	23.02	28.73
14	2	25.98	32.47
14	1	28.16	41.18
15	3	10.62	18.29
15	2	8.62	15.87
15	1	37.67	49.57
16	3	11.10	19.80
16	2	16.24	24.67
16	1	9.10	25.20
17	3	6.55	12.32
17	2	13.12	20.23
17	1	18.91	28.90
18	3	9.10	18.61
18	2	17.25	29.74
18	1	12.81	26.99

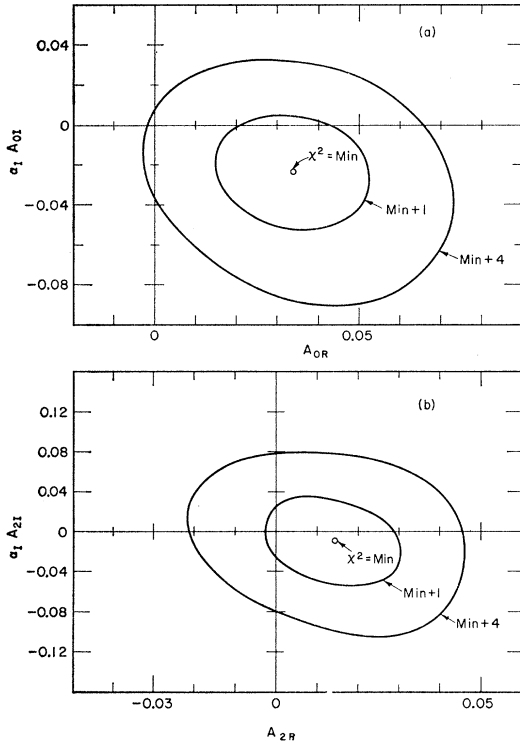


FIG. 5.  $\chi^2$  contour plot for  $C$ -violating parameters. (a) Isospin zero assumed for the three-pion final state. The real part of the  $C$ -violating amplitude,  $A_{0R}$ , is zero in the absence of final-state interactions. The imaginary part of the  $C$ -violating amplitude is  $A_{0I}$ . The imaginary part of the  $C$ -conserving amplitude,  $\alpha_I$ , is zero in the absence of final-state interactions. This plot gives the best-fit values of Eq. (39). (b) Isospin two assumed for the three-pion final state. The real part of the  $C$ -violating amplitude,  $A_{2R}$ , needs final-state interactions to be nonzero. The imaginary part of the  $C$ -violating amplitude is  $A_{2I}$ . This plot gives the best-fit values of Eq. (40).

The best fit is

$$\begin{aligned} \alpha_R &= -0.478 \pm 0.038, \\ \alpha_I^2 &= 0.0025_{-0.1136}^{+0.1467}. \end{aligned} \quad (30)$$

We see that  $|\alpha_I|$  is consistent with zero; it is also consistent with being almost as large as  $|\alpha_R|$ .

We next determine the  $C$ -nonconserving amplitudes. We divide the Dalitz plot into 54 sectors, by subdividing each of our previously considered six sectors into nine regions, as shown in Fig. 1(b). The azimuthal divisions are all 20 deg wide. The radial divisions are chosen at particular (arbitrarily chosen) values of the quantity

$$\rho \equiv p^2 q^2 \sin^2(\theta_{\pi^0 \pi^-}) / p_0^2 q_0^2, \quad (31)$$

where  $p_0$  and  $q_0$  are the values of  $p$  and  $q$  at the center of the Dalitz plot, and  $\theta_{\pi^0 \pi^-}$  is the angle between the  $\pi^0$  and  $\pi^-$  in the  $\pi^+ \pi^-$  frame. At the center of the Dalitz plot (where  $r$  is zero),  $\rho$  is 1;  $\rho$  is zero at the periphery. We choose radial zones No. 1:  $1 \geq \rho > 0.6$ ; No. 2:  $0.6 \geq \rho > 0.3$ ; and No. 3:  $0.3 \geq \rho \geq 0.0$ . The data are shown in Table IX.

In fitting to the data, we assume that *only one* (or the other) of the  $C$ -nonconserving amplitudes  $f_0$  or  $f_2$  is different from zero. The normalization constants  $C$ ,  $c_0$ , and  $c_2$  in Eqs. (23), (25), and (26) are chosen as follows. Let  $N$  be the total number of decays. Then  $C$  is chosen so that the integral over the entire Dalitz plot of the  $C$ -conserving amplitude is given by

$$\iint |F|^2 dx dy = N. \quad (32)$$

When we assume a matrix element  $F + f_0$ ,  $c_0$  is chosen so that

$$\iint |f_0|^2 dx dy = |A_0|^2 N. \quad (33)$$

Thus  $|A_0|^2$  gives the ratio of  $C$ -nonconserving to  $C$ -conserving intensity. Similarly when we assume a matrix element  $F + f_2$ ,  $c_2$  is chosen so that  $|A_2|^2$  gives the ratio of  $C$ -nonconserving to  $C$ -conserving intensity. Thus the calculated number of counts  $dN_c$  in a region  $dx dy$  of the Dalitz plot is given by

$$dN_c = |F + f|^2 dx dy / (1 + |A|^2). \quad (34)$$

For fixed  $y$ , the calculated "left-right excess" is given by

$$dN_c(x) - dN_c(-x) = 4 \operatorname{Re} F^* f dx dy / (1 + |A|^2), \quad (35)$$

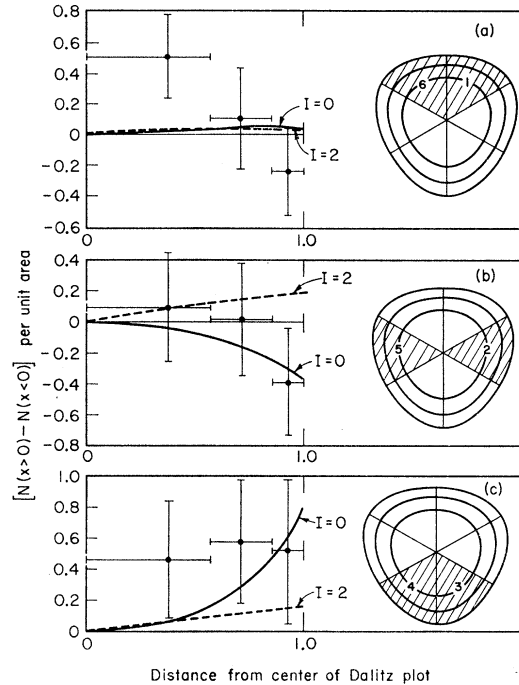


Fig. 6. Charge-asymmetry plots. In each plot the data come from the shaded regions of the Dalitz plot. The charge asymmetry is calculated for each of the three radial zones and is plotted versus fractional distance from the center of the Dalitz plot. The smooth curves correspond to the best-fit parameters of Eqs. (30), (39), and (40).

with

$$\text{Re}F^*f = Cch(x,y)[A_R + y(A_R\alpha_R + A_I\alpha_I)], \quad (36)$$

where  $A$  is  $A_0$  or  $A_2$ ,  $c$  is  $c_0$  or  $c_2$ , and  $h(x,y)$  is  $h_0(x,y)$  or  $h_2(x,y)$ , with

$$h_0(x,y) \equiv x(3y^2 - x^2) \quad \text{and} \quad h_2(x,y) \equiv x.$$

Let  $i$  designate one of the bins having positive  $x$ , occupying a region with (average) values  $r_i$ ,  $\theta_i$ . Let  $j$  designate the corresponding "charge conjugate" bin, with  $r_j = r_i$ ,  $\theta_j = -\theta_i$ . Integrate the right side of (35) over bin  $i$ . The left side of (35) then becomes the calculated "positive excess"  $N_{ei} - N_{ej}$ , expressed in terms of the parameters of physical interest. Let  $N_i - N_j$  designate the observed positive excess as obtained from Table IX. We then form

$$\chi^2 = \sum_{i=1}^{27} \frac{[(N_i - N_j) - (N_{ei} - N_{ej})]^2}{\sigma_{ij}^2}. \quad (37)$$

It would be natural to take  $\sigma_{ij}^2 = (\delta N_i)^2 + (\delta N_j)^2$ , where  $(\delta N_i)^2$  and  $(\delta N_j)^2$  are taken from Table IX. (We neglect the correlation  $\delta N_i \delta N_j$ , since Table VII shows it is comparatively small.) Now,  $(\delta N_i)^2$  is just the corrected number of  $\eta$  decays,  $N_i$ , plus a contribution due to the background subtraction. To smooth the fluctuations, we replace  $N_i$  by the calculated value  $N_{ei}$ . Thus we use

$$\sigma_{ij}^2 = (\delta N_i)^2 + (\delta N_j)^2 + N_{ei} - N_i + N_{ej} - N_j. \quad (38)$$

We vary parameters  $A_R$  and  $A_I$  and make a contour

plot of  $\chi^2$ . Notice that according to Eq. (30),  $\alpha_R$  is very well known, but  $|\alpha_I|$  is very poorly known. Therefore from (35) and (36) we see that we can determine the sign and magnitude of  $A_R$ , but only the relative sign of  $A_I$  and  $\alpha_I$ . In fact, we see that as long as  $|A|^2 \ll 1$  so that the normalization term  $(1 + |A|^2)^{-1}$  in (35) is independent of  $|A|$ , we can only determine the product  $A_I\alpha_I$ .

The  $\chi^2$  contour plots of  $A_R$  and  $A_I\alpha_I$ , for  $A = A_0$  and  $A_2$ , are shown in Fig. 5. The results are

$$\begin{aligned} \text{Isospin zero: } A_{0R} &= +0.034 \pm 0.018, \\ A_{0I}\alpha_I &= -0.022 \pm 0.028, \\ (\chi^2)_{\min} &= 24.0, \quad \langle \chi^2 \rangle = 24 \end{aligned} \quad (39)$$

$$\begin{aligned} \text{Isospin two: } A_{2R} &= 0.014_{-0.017}^{+0.015}, \\ A_{2I}\alpha_I &= -0.010 \pm 0.041, \\ (\chi^2)_{\min} &= 27.1, \quad \langle \chi^2 \rangle = 24. \end{aligned} \quad (40)$$

The fact that  $A_0$  is apparently more significantly different from zero than is  $A_2$  (i.e., two standard deviations as compared to one) reflects the fact that the "alternating" plus-minus asymmetry  $R'$  is more standard deviations from zero than is the asymmetry  $R$ , as we saw in the results (3) and (4).

In Fig. 6 we show the observed plus-minus asymmetry plotted versus  $r$ , together with the predictions from the results (39) and (40), after having integrated over adjacent triplets of azimuthal zones so as to reduce the number of azimuthal zones from 18 to 6.

Our final conclusion is that we need more data.